

20 **ABSTRACT**

21 Worldwide, waste tires are being discarded in landfills at a huge environmental
22 cost, therefore, their use as a three-dimensional reinforcement material is a wise solution
23 to reduce their environmental impact, and fire risk in the case of shredded tires. In this
24 research a series of experimental model tests of embankments reinforced with Geocell
25 and tires were conducted to compare the performance of these types of reinforcement.
26 The models tested had different Geocell embedment depths, number of Geocell layers,
27 vertical spacing between Geocell layers and density or soil stiffness. Testing consisted
28 of applying pressure at the crest of the embankment and monitoring the pressure
29 distribution, as well as the vertical and horizontal deformations inside of the
30 embankment. The results suggested that when compared with unreinforced
31 embankments, reinforced embankments effectively improve the bearing capacity,
32 thereby, reducing vertical and lateral displacements. This study also showed that an
33 optimal embedment depth and spacing between Geocell reinforcement layers can
34 further improve the slope performance. Comparisons between Geocell reinforced
35 embankments and waste tire reinforced embankments, showed that waste tire
36 reinforcement has a superior performance over the Geocell-reinforced embankments.
37 This difference in performance between the two types of reinforcement is more apparent
38 if the embankment backfill has lower stiffness. i.e. lower density.

39

40 **Keywords**

41 Geosynthetics, Soil Reinforcement, Geocell, Waste tires, Bearing capacity, Stress,
42 Settlement, Model Test.

43

44 **1.Introduction**

45 Planar reinforcements (geogrid, geotextiles, wire mesh, etc.) are used to improve
46 soil strength and reduce compressibility (Dash et al. 2007; Soude et al. 2013; Azzam
47 and Nasr 2014; Cicek et al. 2015; Hegde and Sitharam 2015; Xiao and Liu 2016). In
48 recent years research in three-dimensional reinforcement materials (Geocell and waste
49 tires), has shown that this type of reinforcement has a better performance than planar
50 reinforcement, particularly in the case of soft soils. Huang et al. (2001) compared the
51 reinforcement effects of Geocell with those of single and double-layered geogrids,
52 concluding that Geocell reinforcement has better results in terms of deformation
53 mitigation. Latha et al. (2006) and Zhang et al. (2010) have shown that Geocell
54 reinforced embankments have higher bearing capacity and lower settlements, whilst
55 Sitharm et al. (2006) have shown that a foundation reinforced with a geogrid-Geocell
56 composite can better diffuse additional stresses than the Geocell only reinforced
57 foundation.

58 Worldwide, a significant number of waste tires are produced every year and
59 usually sent to landfills at a significant environmental cost. Therefore, numerous
60 researchers are exploring the possibility of using waste tires as reinforcement.
61 Kamarudin et al. (2011) tested a solid tire from 1920s concluding that rubber is highly
62 durable, particularly when not exposed to light and air. Keller (1990) described the use
63 of tire faced retaining walls, which were used effectively to maintain forest roads. Garga
64 and O’Shaughnessy (2000) showed that tire reinforcement can be used with frictional or
65 cohesive soils, providing a satisfactory foundation for medium to light structures. Yoon
66 et al. (2004) and Slack et al. (2008) found that waste tires gave significant
67 improvements in slope stability and bearing capacity. Similar results were observed by

68 Yoon et al. (2008) with tires arranged in an “8” shape. Li et al. (2016) tested the
69 performance of slopes reinforced by waste tires, showing that this type of reinforcement
70 can effectively increase the stability of slopes, reducing deformations. These authors
71 have also shown that the configuration of the tires within the slope is important and can
72 be adjusted to maximize the outcomes.

73 Waste tires can be shredded into sizes of aggregates and used as alternative
74 backfill material (Moghaddas Tafreshi and Norouzi, 2012). Foose et al (1996) have
75 demonstrated that sands reinforced with shredded tires present much higher friction
76 angles than the unreinforced counterpart. Despite the improvements in strength,
77 shredded tires homogeneously mixed in the soil present a much greater combustion risk
78 when used in slope stability than whole tires used as reinforcement layers (Humphrey
79 1996).

80 In this article the behavior of Geocell and waste tire reinforcement under two
81 different backfill densities is compared, emphasizing the effect of the reinforcement on
82 the same soil but with two different stiffnesses. The experimental program also
83 considered factors such as the embedment depth of the Geocell layer, the number of
84 Geocell layers, and Geocell vertical spacing.

85

86 **2. Laboratory study**

87 *2.1. Methodology, Materials and Equipment*

88 Plane strain model scale experiments were conducted inside of a stiff wooden
89 paneled steel frame with plexiglass windows and dimensions of 200 cm (length) × 80
90 cm (width) × 76 cm (height), as shown on Figure 1. Although the results of these tests
91 may be difficult to upscale, the size of the model would be representative of, for

92 example, a strip foundation of a light structure where reinforcement is needed to better
93 distribute the stresses on the soil below; this then avoids plastic deformations by
94 maintaining the soil within the swelling line. Scale tests have many advantages, as they
95 are relatively easy and simple to conduct. Therefore, they offer an excellent chance to
96 test different reinforcement types and configurations, allowing conclusions to be drawn
97 regarding the best options. The influence of the substrate soil was therefore eliminated
98 by constructing the embankment over a stiff base.

99 A cross section of the soil embankment i.e. its dimensions and the arrangement of
100 the instrumentation used are depicted in Figure 2. The angle of the embankment slopes
101 was achieved using suction, by controlling the moisture content of the sand whilst
102 building the embankment. The embankment was built in layers, carefully controlling the
103 weight of wet soil to the volume required by the layer.

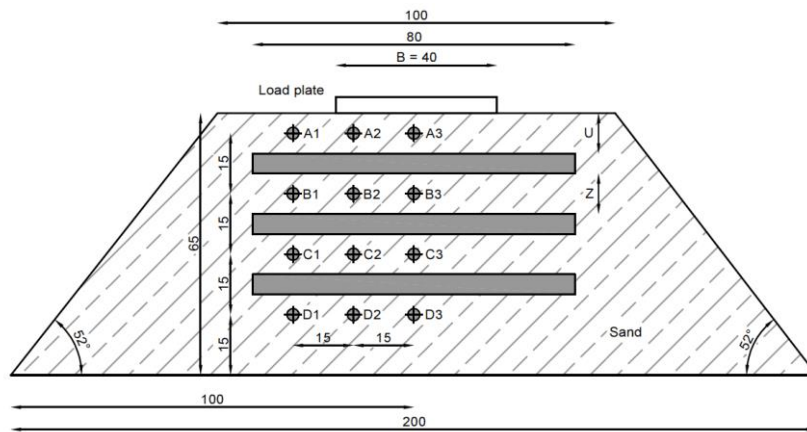
104 A number of steel balls are located adjacent to the plexiglass, at the points where
105 letters represent lines and numbers represent the columns (Figure 2). The movement of
106 these balls was tracked, allowing the measurement of the displacements within the soil
107 mass.

108 A vertical load was applied to the embankment via a loading plate connected to an
109 actuator, and the vertical stress distribution within the embankment was measured by six
110 earth pressure cells located on positions B1, B3, C1, C3, D1, and D3.



111
112
113

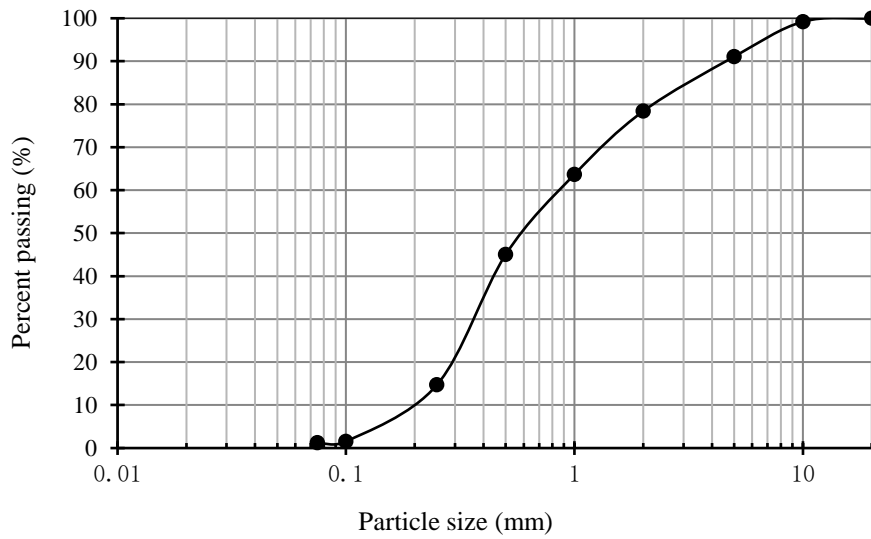
Figure 1 - Test chamber



114
115
116

Figure 2 - Schematics of reinforced embankment systems

117 The materials used in this research include Geocell and waste tires from a local
118 recycling station as reinforcement, and a clean river sand with no fine content. Figure 3
119 shows the particle size distribution curve of the sand used in the experiments. Figure 4
120 shows the pictures taken when the testing embankment was constructed and the
121 reinforcement installed: (a) Geocell reinforcement and (b) waste tire reinforcement. The
122 waste tires were mechanically fastened to each other by high strength friction grip bolts
123 and wires. Tables 1 and 2 list the parameters determined in the laboratory for the sand,
124 the waste tires and the Geocell reinforcement, respectively.



125

126

127

Figure 3 – Grain size distribution of the used sand



128

129

(b) Geocell

(c) Waste tires

130

131

132

Figure 4 – Installation of the reinforcement on the testing embankments: (a) Geocell and (b) waste tires.

133

2.3. Experimental Program

134

135

136

137

138

The experimental program was developed to compare the efficiency of Geocell and waste tires as soil reinforcing agents. Parameters such as the distance between the top surface and the first layer of reinforcement, the distance between reinforcement layers, the number of layers and fill density were analyzed (Table 3).

139

Table 1 - Physical properties of the sand

Parameter	Value
Coefficient of uniformity, C_u	5.4
Coefficient of curvature, C_c	1.4
Maximum dry density (g/cm^3)	1.89
Minimum dry density (g/cm^3)	1.65
Specific gravity, G_s	2.67
Moisture content	6%
Internal angle of friction	35°

140

141

Table 2 – Parameters of the reinforcement

Tires	
Parameter	Value
Diameter (cm)	40
Thickness (cm)	1
Length of the tread (cm)	5
Width of tires sidewalls (cm)	4
Poisson's ratio	0.33
Elasticity modulus (MPa)	2.0×10^3
Geocell	
Height (cm)	5
Length of aperture side (cm)	40
Tensile yield strength (MPa)	24
Tensile modulus (MPa)	6.5
Aperture size (cm)	40 x 40

142

143 To reduce friction a thin layer of lubricant was applied to the lateral panels before
 144 assembling the fill, and each test consisted of the application of a static load to the top
 145 of the embankment via a rigid loading plate (790 mm × 400 mm). The load increments
 146 were equivalent to an increment in vertical stress of 0.5MPa. The experiments were

147 terminated when significant settlement of the loading plate was observed.

148 Table 3 – Configuration and parameters of the model tests

Test No	Reinforcement	Name	<i>U</i> (cm)	<i>Z</i> (cm)	<i>N</i>	<i>Dr</i>	<i>Load</i> (MPa)
1	Unreinforced	Un11	-	-	0	0.11	0.8
2	Geocell	1G125L	0.125B	-	1	0.11	1.28
3	Geocell	1G250L	0.25B	-	1	0.11	1.5
4	Geocell	1G375L	0.375B	-	1	0.11	1.07
5	Geocell	2G125L	0.25B	0.125B	2	0.11	1.8
6	Geocell	2G250L	0.25B	0.25B	2	0.11	2
7	Geocell	2G375L	0.25B	0.375B	2	0.11	1.57
8	Geocell	3G250L	0.25B	0.25B	3	0.11	2.42
9	Unreinforced	Un45	-	-	0	0.45	2.45
10	Geocell	1G250D	0.25B	-	1	0.45	2.72
11	Waste tire	1T250D	0.25B	-	1	0.45	3.32
12	Waste tire	1T250L	0.25B	-	1	0.11	2.07

149 **Note:** *U*: Distance from the embankment crest to the first reinforcement layer; *Z*: vertical spacing between
150 reinforcement layers; *N*: Number of reinforcement layers; *Dr*: relative density of soil. *Load* is the load required for a
151 vertical displacement $s/B=3\%$. *U* and *Z* are illustrated in Figure 2. Name: Un – Unreinforced; G – Geocell; T – tire; D
152 – denser ($Dr=45\%$); L – loose ($Dr=11\%$); 125, 250 and 375 – distance between the last layer and the surface of the
153 embankment or the previous layer, equal to = 0.125B, 0.25B and 0.375B, respectively.
154

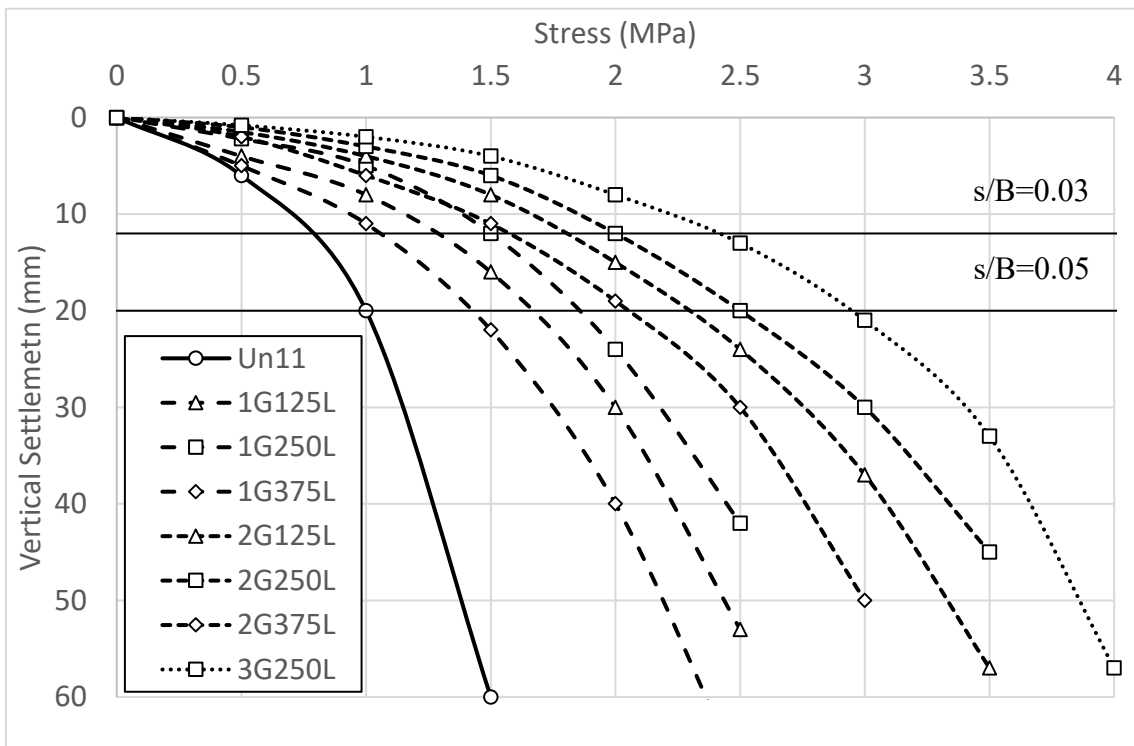
155

156 3. Test Results

157 3.1. Load versus settlement

158 Figure 5 shows the load-settlement curves (p-s curves) obtained from tests
159 performed on the unreinforced embankment and Geocell reinforced embankments
160 (Table 4, tests 1 to 8). As seen in the figure, the settlement of all the tested embankments
161 increased with an increase in pressure. The settlement ratio also increased gradually
162 with the load applied, generating larger and larger plastic strains at every increment of
163 load. As the settlement of the embankment increased, cracks started appearing at the

164 surfaces. For the case of the unreinforced embankment, cracks started appearing when
 165 the ratio between the settlement (s) and the width of the foundation or loading plate (B)
 166 was around 3% ($s/B=0.03$). The reinforced slopes showed cracks being formed once the
 167 settlement reached a larger value, 5% ($s/B=0.05$). Therefore, the load corresponding to a
 168 settlement of 3% was used for performance comparisons.



169
 170 **Figure 5 - Effect of reinforcement depth and the number of layers on the**
 171 **pressure-settlement curves for the slopes with a $Dr=11\%$.**
 172

173 All reinforced slopes have shown a better performance than the unreinforced
 174 slope. The test results also show that there is an optimum depth for the location of the
 175 reinforcement layer: as the depth increases from 0.125B to 0.25B, the bearing capacity
 176 increases. However, when the depth is increased to 0.375B, the bearing capacity
 177 reduces, indicating that the optimum depth is located around 0.25B. A similar behavior
 178 can be seen for the embankment reinforced with 2 layers of Geocell, where the first
 179 layer was kept at 0.25B from the embankment surface. As the distance between the first

180 and second layer increased from 0.125B to 0.25B, the stiffness and the ultimate load
181 also increased. However, as this distance is increased from 0.25B to 0.375B, the
182 stiffness and ultimate load reduced to values that are lower than the embankment with
183 0.125B between the first and the second layers.

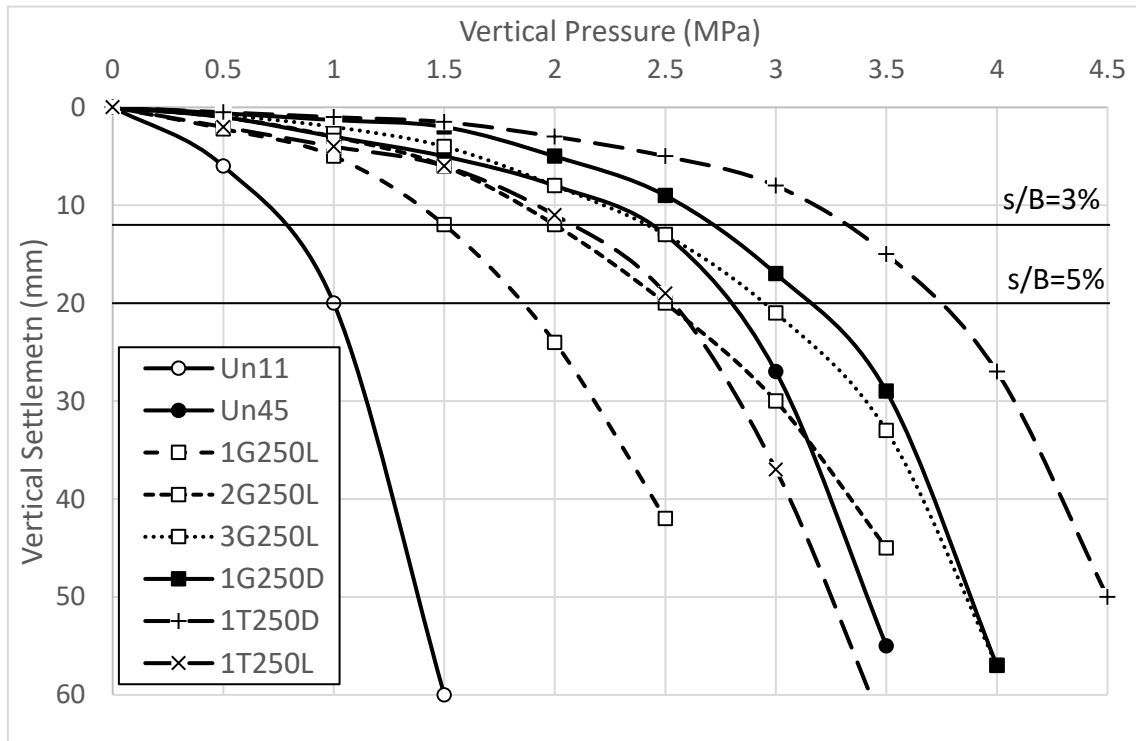
184 The addition of a third reinforcement layer of Geocell yields a further
185 improvement in stiffness and ultimate strength, however, the gain with respect to the
186 embankment reinforced with two layers is reduced. At a value of $s/B=3\%$, Un11 reached
187 a vertical stress of around 0.77MPa and the embankment 1G250L a vertical stress of
188 1.5MPa. The addition of one layer of reinforcement was then seen to almost double the
189 performance of the embankment. With the addition of a second layer of reinforcement at
190 $s/B=3\%$, the load increased to 2MPa, giving an improvement of 0.5MPa or 33%. With
191 the addition of a 3rd layer, the load at $s/B=3\%$ further increased to 2.4MPa, yielding an
192 increase of 20% when compared to the embankment reinforced with 2 layers.

193 The test results show clearly that there is an optimum depth for the location of
194 every layer of reinforcement, and for the tests presented in Figure 5, at the lowest
195 relative density this distance is 0.25B. These are likely to depend on the thickness and
196 stiffness of the reinforcement, as well as on the friction and stiffness properties of the
197 soil, or the density achieved during compaction.

198 The test results related to the best location of the first layer of Geocell
199 reinforcement (0.25B in this study) are different than those obtained by Yoon et al.
200 (2008) and Li et al. (2016) for tire reinforcement. These authors demonstrated that for
201 tire reinforcement the location of the first layer should be as close as possible to the
202 location of the loading application on the embankment.

203 In Figure 6 the load settlement curves of both unreinforced embankments, the Geocell

204 reinforced embankments, and the tire reinforced embankments are plotted together
 205 (Table 4, tests 1, 3, 6, 8 and 9 to 11). These tests were performed based on the results of
 206 the previous tests, i.e. using the distance between layers that yielded the highest
 207 embankment strength or 0.25B. Un45 is an unreinforced embankment with a relative
 208 density of 45%, showing an initial behavior similar to test 3G250L up to a ratio $s/B=3\%$
 209 and losing strength quickly afterwards. The embankment reinforced with one layer of
 210 tires and a low relative density (1T250L) had a performance similar to the embankment
 211 reinforced with 2 layers of Geocell; this shows that tires offer a better alternative to the
 212 use of Geocell in terms of performance. The same behavior was observed when
 213 comparing the reinforced embankments using the densest configuration, where a layer
 214 of tire reinforcement offers better performance than the Geocell. In the tests performed
 215 the strength improvement against Geocell is around 23% (from 2.70 to 3.32MPa).



216

217 **Figure 6 - Effect of the type of reinforcement and the Relative density on the**
 218 **pressure-settlement curves.**

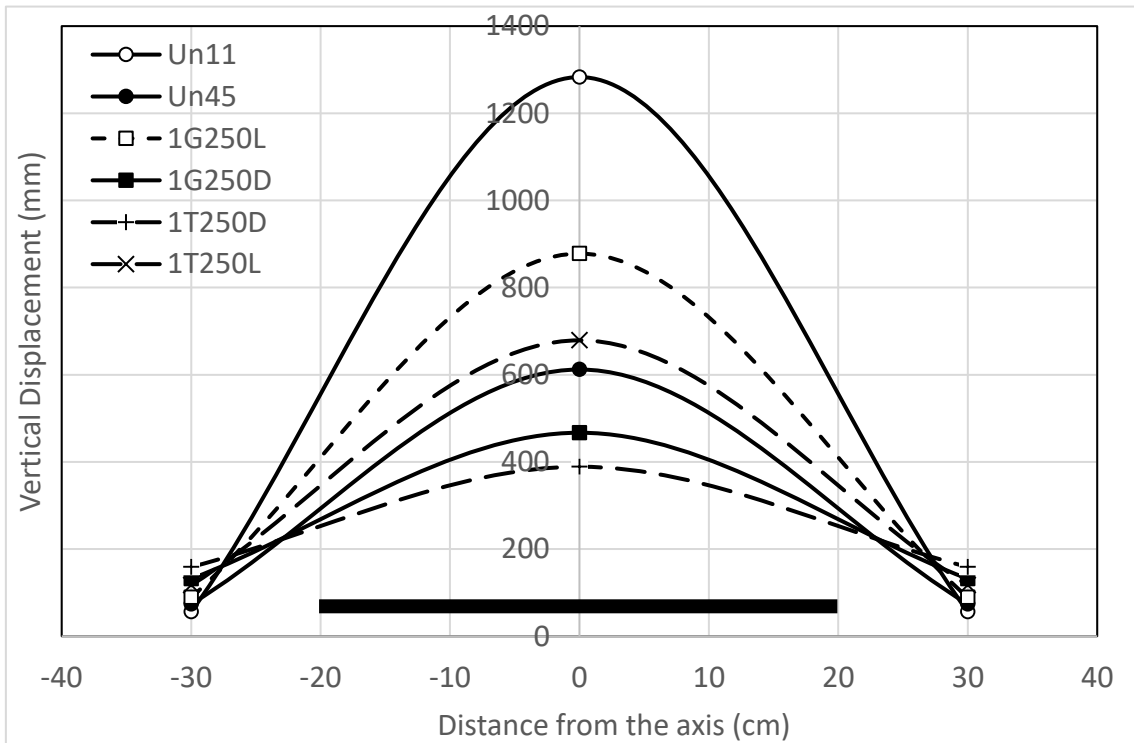
219 It is also noticeable that the improvement in performance amongst the denser
220 embankments is not large when compared to the unreinforced soil. It is seen that one
221 layer of Geocell improves the performance by around 10%, whilst a layer of tire
222 reinforcement by 35%. Better improvement in the performance is seen when the soil is
223 of a lower density (lower stiffness); where a performance increase of 87.5% for Geocell
224 and 158% for tire reinforcement was measured. The improvement must, therefore, be
225 related to the stiffness of the reinforcement. Therefore, the highest increase in strength is
226 seen in the stiffer reinforcement of the tires, and as the stiffness of the soil increases
227 with density, the effectiveness of the reinforcement is reduced.

228 ***3.2 Stress distribution***

229 To understand the changes in stress distribution caused by the addition of
230 reinforcement, the pressure values measured at positions B1 and B3 (Figure 2) were
231 plotted in Figure 7 against the distance from the vertical axis, for a vertical pressure of
232 1.5MPa. Given the symmetry of the model embankment, the value at B3 was mirrored
233 along the central axis of the embankment. Also represented in the figure is the loading
234 plate, centered on the vertical axis. For all tests, the highest vertical pressure is
235 measured at the vertical axis, reducing to much smaller values 30cm away (the loading
236 plate only extends up to 20cm away from the axis), therefore, not all test results were
237 plotted in the figure.

238 The unreinforced tests (Un11 and Un45) have the highest pressures at the axis
239 center line for the density tested. However, the highest density (Un45) showed a lower
240 value of vertical stress at the vertical axis of the embankment than the lowest density
241 (Un11). The opposite was seen at 30cm from the axis where Un45 showed higher
242 stresses than Un11; this is likely to be caused by a type of failure similar to a rigid

243 punch, commonly seen on soft soils. The addition of reinforcement reduced the
 244 pressures measured at the center line, however, the highest reduction is seen for the tire
 245 reinforcement. At location B3 the values are inverted, i.e.: the highest stress is measured
 246 in the embankment reinforced with tires. This shows that the reinforcement is
 247 mobilizing soil strength further away from the influence of the loading plate, reducing
 248 the maximum stresses measured under the center axis, and spreading the stresses over
 249 large volumes of soil. The same can be seen for the reinforced embankments created
 250 with a relative density of 45%, where the highest reduction in vertical stress was seen
 251 along the central axis or point B1. Whilst at point B3, the tire reinforced slope caused
 252 the highest vertical stress measured, followed by the embankment reinforced with
 253 Geocell, indicating a more homogeneous stress distribution even further away from the
 254 edges of the load application plate.



255

256 **Figure 7 – Stress distribution at 20cm below the embankment surface for a 1.5MPa**
 257 **applied pressure, at the surface. The black line indicates the size and location of**

258 **the loading plate.**

259

260

Again, this shows the effectiveness of the reinforcement in reducing the higher

261

stresses acting in the soil mass, as well as the mobilization of strength in larger volumes

262

of soil. The results are proportional to the overall stiffness of the reinforcement plus

263

soil. The higher the overall stiffness, the more homogeneous the distribution of stresses

264

in the soil; in these tests this is achieved by either the addition of the reinforcement or

265

the compaction of the soil (density).

266

267

3.3 Vertical and horizontal Deformations

268

Figure 8 shows the settlement at locations B1, B2 and B3 for the same tests as

269

Figure 7, however, the vertical load applied on the denser tests is of 3MPa. As before,

270

given the symmetry, the results were mirrored to give a full plot of vertical

271

displacements at the location mentioned above. Between the unreinforced

272

embankments, as expected Un11 showed much higher vertical displacements than

273

Un45, despite the load being applied at Un45 being twice of that at Un11. With the

274

addition of reinforcement there is a reduction in the settlement level, and this reduction

275

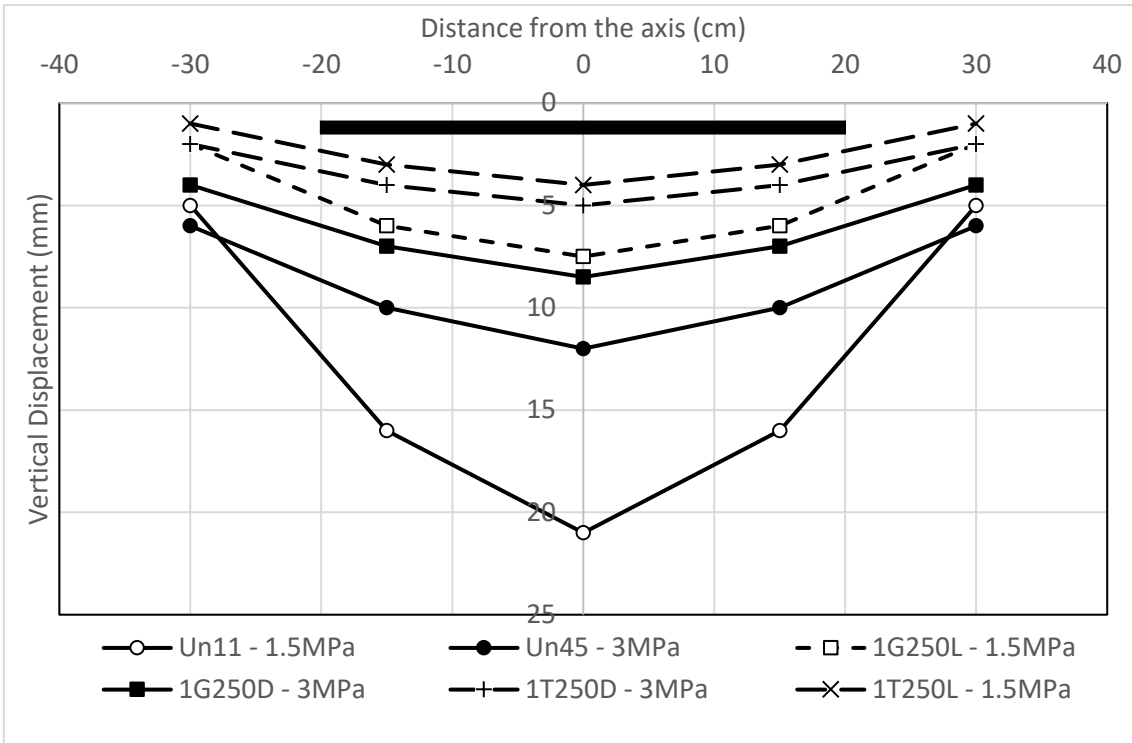
is larger for the lower density embankments. It is also possible to see that the vertical

276

displacements of the embankments reinforced with tires present much lower vertical

277

deformations than the Geocell reinforcement.

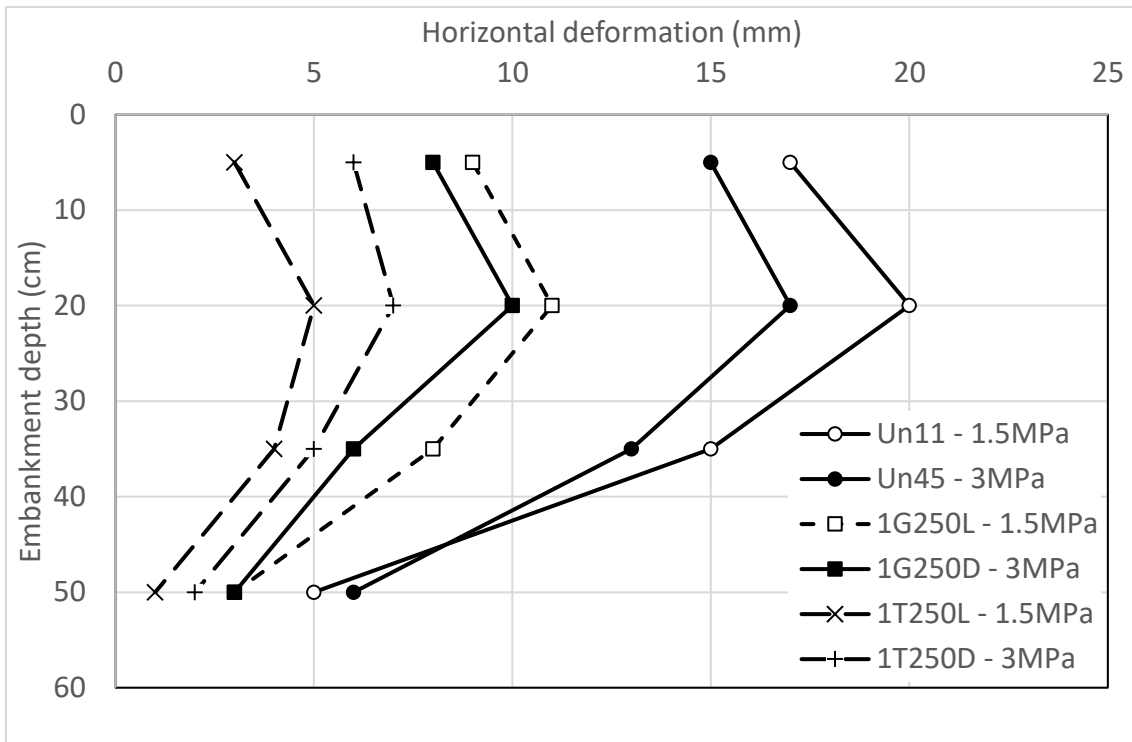


278

279 **Figure 8 – Settlement distribution inside the embankment for a vertical pressure of**
 280 **1.5MPa for the loose embankment and 3MPa for the dense embankment. Black line**
 281 **indicates the size and location of the loading plate.**

282

283 The horizontal deformations of points A1, B1, C1, and D1 were also measured and
 284 plotted in Figure 9 for the same tests. Again, for the denser embankment the horizontal
 285 deformations measured corresponded to a vertical stress of 1.5MPa, whilst the denser
 286 embankments were subjected to a vertical stress of 3MPa.



287

288 **Figure 9 – Horizontal deformation of the embankment for a vertical pressure of 1.5MPa**
 289 **applied on the loose embankments ($D_r=11\%$) and 3MPa on the dense embankments**
 290 **($D_r=45\%$).**
 291

292 Similar to what was seen before, the unreinforced slopes showed very large lateral
 293 deformations for the applied vertical stress. The larger lateral deformations were
 294 observed in the loose unreinforced embankment despite the load applied being only half
 295 of the one applied in the dense embankment. The addition of reinforcement drastically
 296 reduced the lateral deformation of the embankment, and the tire reinforcement showed
 297 better performance than the Geocell reinforcement.

298 The large change in behavior is seen for the maximum vertical deformation,
 299 where the use of Geocell reinforcement generated a vertical settlement of around 36%
 300 of the settlement of the unreinforced embankment. The use of tires however, generated
 301 around 19% of the settlement. For the densest embankment the values measured were
 302 around 71% and 42% respectively. The values obtained for the lateral displacement

303 were somewhat similar, 55% for Geocell reinforcement and 25% using tire
304 reinforcement on the loosest embankments, whilst the densest showed 59% and 41%,
305 respectively.

306

307 **4. Conclusions**

308 The outlined experimental results were performed to analyze the effect of the depth of
309 the reinforced layers on the mechanical properties of a model embankment. The
310 performance of Geocell reinforcement to a more environmentally friendly alternative
311 were also compared, and the results have shown that:

- 312 • The performance of the model embankment is dependent on the depth of the
313 first reinforcement layer and the distance between reinforcement layers. The
314 study of the Geocell reinforced embankment presented here has demonstrated
315 that the optimum depth for the first layer is $0.25B$, and that the distance between
316 layers is also $0.25B$.
- 317 • Increasing the number of reinforcement layers improves the mechanical
318 properties of the model embankment, however, the improvement is reduced with
319 the addition of each extra layer, alluding to the existence of a limited number of
320 reinforcement layers.
- 321 • The reinforcement can be used to effectively reduce the maximum vertical stress
322 seen on the embankments, as well as to create a more homogeneous stress
323 distribution, that will in turn generate lower settlements and lower horizontal
324 deformations.
- 325 • For loose embankments the improvements observed by using Geocell or waste
326 tire reinforcement are better than the improvements observed in the densest

327 embankments. This confirms that the application of these types of reinforcement
328 are best suited for soft or loose soils.

- 329 • For the configurations used in the experiments waste tire reinforcement has
330 outperformed Geocell reinforcement in both stress and deformation reduction, it
331 is also a more environmentally friendly alternative to reinforcement.

332

333 **Acknowledgements**

334 The authors are thankful for the financial support given by the Hubei Provincial
335 Science Foundation for Distinguished Young Scholars (No. 2018CFA063); the National
336 Natural Science Foundation of China (No.51678224, 51778217); the National Program
337 on Key Research Project of China (No. 2016YFC0502208) and Hubei Central Special
338 Fund for Local Science and Technology Development (No.2018ZYD005).

339

340 **References**

341 Alamshahi, S., and Hataf, N. (2009). Bearing capacity of strip footings on sand slopes
342 reinforced with geogrid and grid-anchor. *Geotextiles and Geomembranes*. 27,
343 217-226.

344 Azzam, W.R., and Nasr, A.M. (2015). Bearing capacity of shell strip footing on
345 reinforced sand. *Journal of Advanced Research*. 6, 727-737.

346 Cicek, E., Guler, E., and Yetimoglu, T. (2015). Effect of reinforcement length for
347 different geosynthetic reinforcements on strip footing on sand soil. *Soils and*
348 *Foundations*. 55, 661-677.

349 Dash, S.K., Rajagopal K., and Krishnaswamy, N.R. (2004). Performance of different
350 geosynthetic reinforcement materials in sand foundations. *Geosynthetics*

351 International. 11, 35-42.

352 Dash, S.K., Rajagopal K., and Krishnaswamy, N.R. (2007). Behavior of Geocell-
353 reinforced sand beds under strip loading. *Canadian Geotechnical Journal*. 44, 905-
354 916.

355 Foose G.J., Benson G.H., Bosscher P.G. (1996). Sand reinforced with shredded waste
356 tires. *Journal of Geotechnical Engineering* 122, 760–767.

357 Garga, V.K.; O’Shaughnessy, V. (2000). Tire-reinforced earth fill. Part 1: Construction
358 of a test fill, performance and retaining wall design. *Canadian Geotech. Journal*.
359 37, 75–96.

360 Huang, G., Zhang, Q., Yu, X, Luo, Q., and Cai, Y. (2001). Comparison of settlement
361 control of reinforcement layer. *Chinese Journal of Geotechnical Engineering*. 23,
362 598-601. (in Chinese).

363 Hegde, A, and Sitharam, T.G. (2015). 3-Dimensional numerical modelling of Geocell
364 reinforced sand beds. *Geotextiles and Geomembranes*. 43, 171-181.

365 Humphrey, D. N. (1996). Investigation of Exothermic Reaction in Tire Shred Fill
366 Located on SR 100 in Ilwaco, Washington. Report Prepared for Federal Highway
367 Administration, March 1996.

368 Kamarudin, S.; Le Gac, P.-Y.; Marco, Y.; Muhr, A.H. Formation of crust on natural
369 rubber after ageing. In *Proceedings of the 7th European Conference on*
370 *Constitutive Models for Rubber*, ECCMR, Dublin, Ireland, 20–23 September
371 2011; pp. 197–202, doi:10.1201/b11687-37.

372 Keller, G. R. (1990). Retaining Forest Roads. *Civil Engineering – ASCE*. 60, 50-53.

373 Krishnaswamy, N.R., Rajagopal K., and Madhavi Latha, G. (2000). Model studies on
374 Geocell supported embankments constructed over a soft clay foundation.

375 Geotechnical Testing Journal. 23, 45-54.

376 Latha, G.M., Rajagopal, K., and Krishnaswamy, N.R. (2006). Experimental and
377 theoretical investigations on Geocell-supported embankments. International
378 Journal of Geomechanics - ASCE. 6, 30-35.

379 Li, L.H., Xiao H.L., Ferreira, P., and Cui, X. (2016). Study of a small scale tyre-
380 reinforcement embankment. Geotextiles and Geomembranes. 44, 201-208.

381 Moghaddas Tafreshi, S.N. and Norouzi, A.H. (2012). Bearing capacity of a square
382 model footing on sand reinforced with shredded tire-An experimental
383 investigation. Construction and Building Materials. 35, 547-556.

384 Sitharm, T.G. and Sireesh, S. (2006). Effects of base geogrid on Geocell-reinforced
385 foundation beds. Geomechanics and Geoengineering. 1, 207-216.

386 Slack, D. C., Garcia, G., Roth, R., Hoenig, S., Segovia, R., Soto, R. & Frayre, A.
387 (2008). Engineered Conservation Structures using Discarded Tires. In American
388 Society of Agricultural and Biological Engineers - Conference on 21st Century
389 Watershed Technology: Improving Water Quality and Environment, Concepcion,
390 Chile, March 29 – April 3, 2008. 163-170.

391 Soude, M., Chevalier, B., Grediac, M., Talon, A., and Gourves, R. (2013). Experimental
392 and numerical investigation of the response of Geocell-reinforced walls to
393 horizontal localized impact. Geotextiles and Geomembranes. 39, 39-50.

394 Tafreshi, S.N.M. and Dawson, A.R. (2012). A comparison of static and cyclic responses
395 of foundations on Geocell reinforced sand. Geotextiles and Geomembranes. 32,
396 55-68.

397 Xiao, H. and Liu, Y. (2016). A prediction model for the tensile strength of cement-
398 admixed clay with randomly orientated fibres. European Journal of Environmental

399 and Civil Engineering. 22, 1131-1145.

400 Yoon, Y.W., Cheon, S.H., and Kang, D.S. (2004). Bearing capacity and settlement of
401 tire-reinforced sands. Geotextiles and Geomembranes, 22, 439-453.

402 Yoon, Y.W., Heo, S.B., and Kim, K.S. 2008. Geotechnical performance of waste tires
403 for soil reinforcement from chamber tests. Geotextiles and Geomembranes. 26,
404 100-107.

405 Zhang, L., Zhao, M., Shi, C., and Zhao, H. (2010). Bearing capacity of Geocell
406 reinforcement in embankment engineering. Geotextiles and Geomembranes. 28,
407 475-482.

408 Zhang, Z.F, Liu, SY, Cai, G.H, Wei, Q.B. (2015). Research progress of scrap tires used
409 in road engineering. China Civil Engineering Journal. 48:S2, 361-368.

410